11 Spatial analysis of wind shelterbelt effects: a model for regional planning

Roger Funk [1,*], Lidia Völker [1], Florian Kestel [1], Maik Veste [2,3], Tobias Hahn [4]

[1] Leibniz Centre for Agricultural Landscape Research (ZALF e.V.), Eberswalder Str. 84, 15374 Müncheberg, Germany

[2] CEBra - Center for Energy Technology Brandenburg e.V., Cottbus, Germany.

[3] University of Hohenheim, Institute of Biology, Department Molecular Botany, Stuttgart, Germany

[4] Orchard Research Station Müncheberg (OBVS), Müncheberg, Germany

* corresponding author: rfunk@zalf.de

ORCID Roger Funk 0000-0001-8739-6201

ORCID Maik Veste: 0000-0003-2704-2588

Abstract

Keywords: landscape structure, wind velocity reduction, wind erosion, potential evapotranspiration, water saving

11.1 Introduction

Agriculture and food security are facing major challenges due to global change worldwide. This puts increasing pressure on the efficient use of limited land and resources to ensure stable agricultural production (Rötter et al. 2014) and avoid conflicts with other livelihoods and economies (Snyder et al. 2015). This is being exacerbated by climate change, particularly in the form of rising temperatures, changes in precipitation patterns, heat waves and droughts, which will ultimately lead to water scarcity for crops and increased yield uncertainty (Brune 2016, IPCC 2021, von Maltitz et al. 2014). This particularly affects the semi-arid regions where evaporation exceeds the amount of precipitation. Protecting the soils against degradation by erosion and saving water are therefore an absolute necessity for successful and efficient agriculture. All available potentials should be used for this purpose, preferably those that generate positive effects through their presence alone. This applies to the landscape structure, as it is well known that a structured landscape has wind reducing, shading and cooling effects. So, landscape structures combine many positive effects (Chapter 14) by reducing soil erosion, creating safe habitats for plants and animals and thus increase biodiversity, connecting biotopes or simply determining the aesthetics of a landscape (Vigiak et al. 2003, Pásztor et al. 2016, Sheppard et al. 2020).

Wind erosion is a gradual soil degradation process characterized by the removal of the finest and lightest particles, such as the clay and silt fractions and the soil organic matter (SOM). Over time, this leads to a deterioration in the physical and chemical properties of the soils (Goossens 2004, Borelli et al. 2017, Nerger et al. 2017). This is a particular problem in semi-arid regions with agricultural use, but temperate latitudes are also increasingly confronted with this problem (Reich et al. 2001, Zolina et al. 2013). The classification of the wind erosion risk of larger areas is usually based on the spatial distribution of soil types and wind velocities (e.g. for South Africa Kestel et al. 2023, Zhao et al. 2021). The effect of vegetation on the wind erosion risk is included as displacement height and aerodynamic roughness length, but only related to the place of its presence (Funk and Reuter, 2006; Borelli et al., 2014, Borelli et al., 2017). The fact that the influence of forests, hedges, shrubs and other landscape structures can be up to 40 times of their height is hardly taken into account in large-scale analyses (Hagen et al., 1981, van Eimern, 1964, Vigiak et al. 2003).

The water balance of soils is primarily dependent on intrinsic factors such as soil texture, soil organic matter content or bulk density, which determine the water holding and water transport capacities directly at the site (Horton et al. 2016, Jacobs et al. 2022, Veste et al. 2020). In heterogeneous landscapes the spatial pattern of soils, topography and land use determine spatial differences in water availabilities (Schmidt et al. 2004). However, in the landscape context, also other factors contribute to this, which can be attributed to micrometeorological effects, mainly related to evapotranspiration (Allen at al. 1998, see chapter 5, 10). This is particularly relevant for landscape elements as small forests, shelterbelts, trees or shrubs that influence directional meteorological parameters such as wind velocity or solar radiation and results in windward and leeward effects or sunny and shady sides in close proximity to each other. This causes further spatial differences of temperature, humidity, evaporation or dew formation, and different growth conditions for crops between both sides which go far beyond the effects at the location. Many micrometeorological measurements have been carried out around windbreaks in recent decades (Caborn 1957; Plate 1971; Schwartz et al. 1995; Cleugh 1998; Cleugh and Hughes 2002, Vigiak et al. 2003; Böhm et al. 2014; Kanzler et al. 2019; Weninger et al. 2022), quantifying these effects which can result in different growing conditions and yields of agricultural crops finally (Baker et al. 2016, Schmidt et al. 2019, Baker et al. 2021, chapter 13)

In the case study we illustrate the influence of landscape elements on the spatial variability of the directional meteorological parameter wind velocity and how that affects the reduction of the wind erosion risk and the potential evapotranspiration. Our analysis is intended for larger regions and was therefore integrated into a GIS (Funk and Völker 2024). The ArcGIS toolbox "WERA" should help to identify problem areas of wind erosion within the region and to illustrate differences in water availability between or within fields in a quantitative way. The approach can be transferred also to other regions like Southern Africa, where wind erosion is a major threat for agriculture and land-uses (Kestel et al. 2023, Baade et al. 2024) for regional and local planning.

11.2 Toolbox "WERA"

Our methodology is based on the ArcGIS toolbox "WERA", which was developed to assess the influence of landscape elements on the wind erosion risk by shadowing effects (Funk et al. 2023, Funk and Völker 2024). The model calculates the reduction of the wind erosivity based on the frequencies of wind velocities above a certain soil specific threshold and their directional distributions. For this purpose the location and height of all landscape elements are required. This information can be obtained from maps, on-site measurements or remote sensing methods as laser scanning.

Since the reduction in wind speed not only affects wind erosion, but also has an impact on other micrometeorological parameter as the evapotranspiration, this approach can also be used for this purpose. The aim here was to show how the wind reducing effects of LE influences this parameter in its spatial variability and to estimate water-saving effects. In this way, shorter periods of time or individual events can be calculated.

11.2.1 Landscape structure

The landscape structures (Fig. 11.1) for the purposes of this study are needed as information about height and spatial arrangement of each landscape element (LE). We derived a landscape structure model from an aircraft-based laser scanning campaign for the Digital Elevation Model (DEM), where the surface and all objects on it were scanned in a grid with a horizontal resolution of 1 x 1 m and a vertical resolution of ± 0.25 m (LGB 2020). The laser scanning resulted in two layers, the Digital Surface model (DSM), including everything with a certain height, and the derived Digital Elevation Model (DEM), representing the land surface after eliminating all landscape elements as buildings or vegetation. The height of any landscape element can be received by subtracting the DEM from the DSM. This step eliminates topography and the resulting new layer includes only the measured landscape elements on a flat surface. Additionally, all height values inside of agricultural land were set to zero using the structures of a Digital Field Block Cadastre (DFBK, LGB 2023), because temporary silos or hay bales left in the fields were also measured by the laser scanning during the overflight.

Figure 11.1. Landscape elements at the study site of Orchard Research Station, Müncheberg, Brandenburg

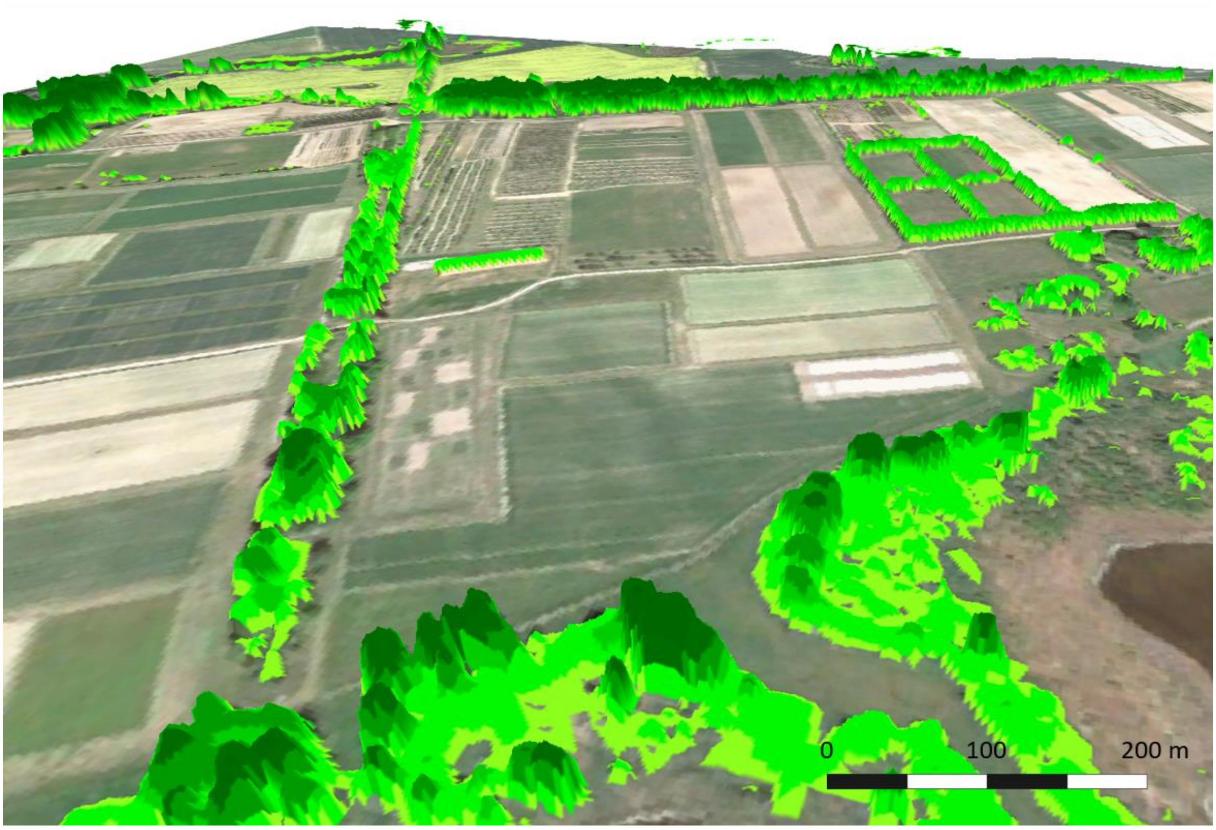

Figure 11.2. Landscape unit with all scanned landscape elements at the study site of Orchard Research Station, Müncheberg, Brandenburg

The decrease in wind speed behind windbreaks is well studied and shows a distinct decrease on the leeward site at first, which then gradually increases back to the original value with increasing distance. One of the few mathematical descriptions of this curve can be found in the WEPS model (Hagen and Fox 2020). The equation calculates the decrease and increase of the wind speed behind the LE as multiples of its height (Eq. 1, Fig. 11.3). Also the porosity (p) of the windbreak can be entered as an additional parameter (Eqs. 2 - 5). An average value is sufficient for the evaluation of long-term effects; if the method is used on an event-related basis, it is possible to react to the different foliage in winter or summer.

$$fu = 1 - \exp(-m * x^2) + n * exp(-0.003(x + s)^t) \quad (1)$$

where

fu wind reduction factor

x distance from the structure element in multiples of height.

The coefficients m, n, s and t depend on porosity (p) and are calculated as follows

$$m = 0.008 - 0.17p + 0.17p^{1.05} \quad (2)$$

$$n = 1.35(-0.5p^{0.2}) \quad (3)$$

$$s = 10\,(1-0.5p) \tag{4}$$

$$t = 3 - p \tag{5}$$

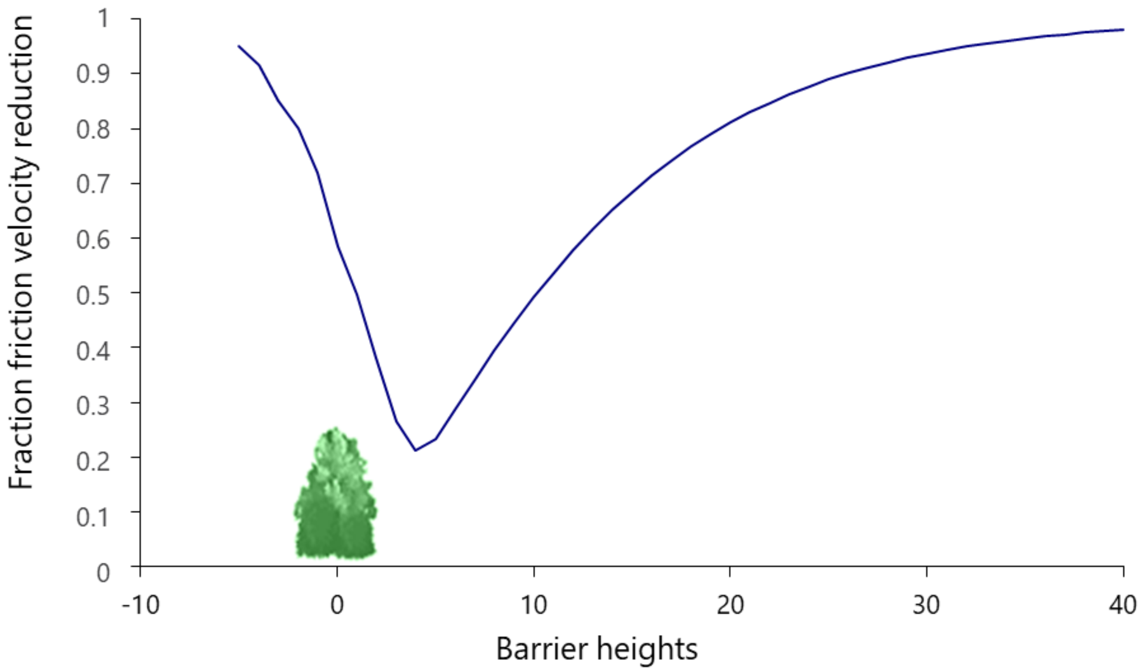

Figure 11.3 Wind velocity reduction in front and behind a wind barrier in multiples of the barrier heights calculated with equations 1- 5 for a porosity of 40 per cent

11.2.2 Meteorological data

Our study uses hourly data of temperature, precipitation, global radiation, air humidity, wind velocity and wind directions available from 1991 to 2023. The data were obtained from DWD Climate station in Müncheberg (DWD Climate Data Centre, DWD station 3376, 14.12 E, 52.52 N). The data were used to calculate the wind erosivity, the sheltering distance behind the LE for all wind directions and the potential evapotranspiration (PET) for each hour of that period.

Derivation of parameters influencing wind erosion

The wind erosivity and the wind directions are the basis to derive an effective sheltering distance behind any LE for all measured directions. First, the frequency distribution of measured winds (u) above a threshold wind velocity (u_t) and the transport capacity q (Eq. 1) were used to calculate a weighted transport capacity for each direction (Fig. 11.4):

$$q = (u - u_t)^2 \qquad \text{for } u > u_t \tag{1}$$

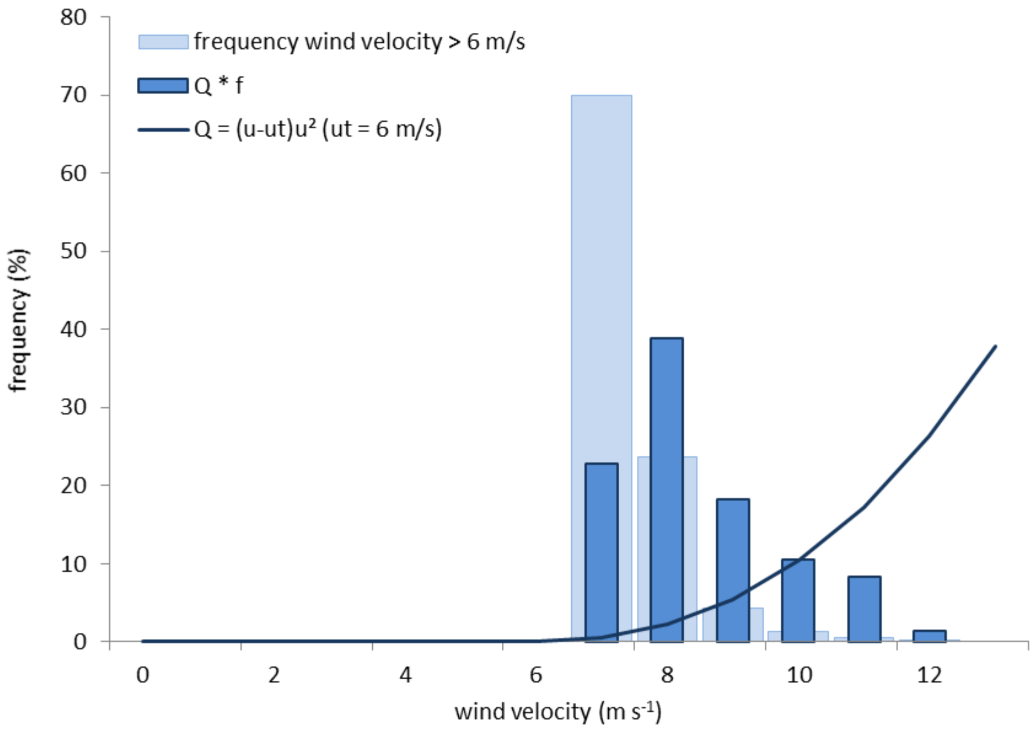

Figure 11.4 Frequency of hourly wind velocities above the threshold of 6 m s^{-1} (light blue bars); transport capacity of the wind based on the relationship $q = (u - u_t)u^2$ (black line); relative transport capacity q*f (blue bars) (Funk et al. 2023)

Generally, the wind reducing influence of a windbreak is indicated with the 40-fold of its height, which refers to the initial level. If a threshold velocity is set, this distance only applies to this velocity. Higher velocities result in shorter distances, so that exceeding this threshold value reduces the protective distance (Fig. 11.5). From the combination of the relative transport capacities and the effective protection distance derived for each wind velocity level, new weighted protection distances can be calculated for each wind direction (Table 11.1).

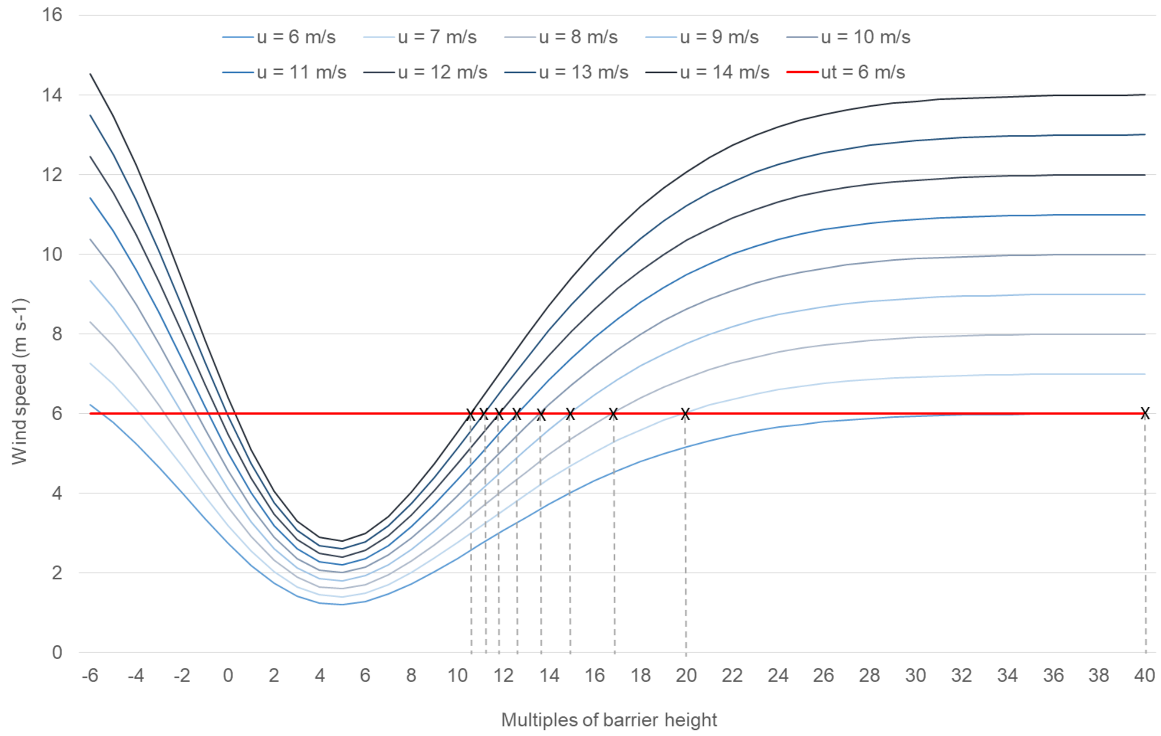

Figure 11.5. Wind velocity reduction in front and behind a landscape element for wind velocities above a threshold; red line marks the threshold wind velocity for wind erosion on sandy soils, the crosses mark the distances from which the wind velocity becomes erosive again

Table 11.1. Example for the derivation of the effective protection zone behind a landscape element, taking into account the transport capacities of all occurring wind velocities above the threshold

Wind velocity class	(A) relative transport capacity (%)	(B) class middle in multiples of height	A * B **Σ/100**
6 - 7 m s^{-1}	22.9	28	641.2
7 - 8 m s^{-1}	38.8	17.5	679.0
8 - 9 m s^{-1}	18.2	15	273.0
9 - 10 m s^{-1}	10.5	12.8	134.4
> 10 m s^{-1}	9.6	10	96.0
			18.2

This is made for each considered wind direction separate. The result is then the effective protective length of a wind barrier in the corresponding direction, expressed in multiples of the height of the LE. In a final step, these effective protection lengths of each direction are then multiplied by the normalized transport capacity of each direction. The direction with the maximum transport capacity is given a factor of 1, all others are reduced accordingly (Fig. 11.6, right).

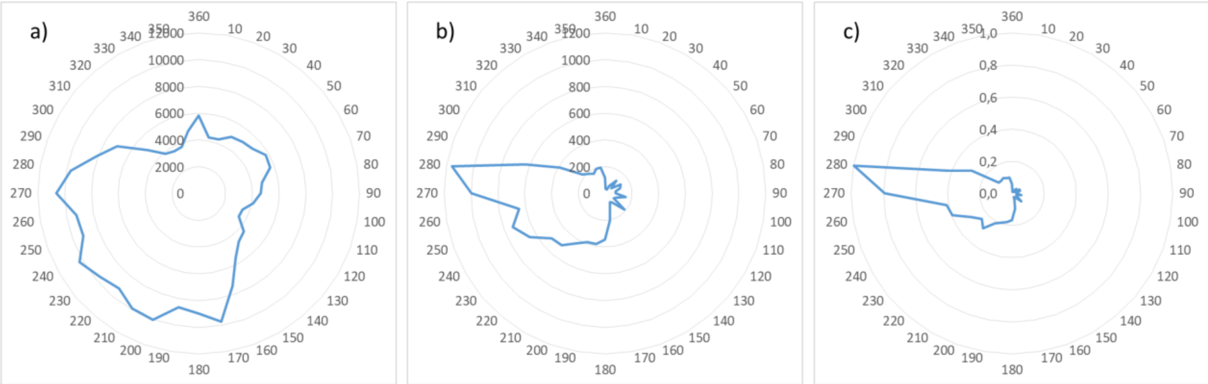

Figure 11.6. Wind speed distributions: a) all wind speeds (hours), b) wind speeds above the threshold of 6 m s^{-1}(hours), and c) relative transport capacities of each direction (normalized, maximum = 1)

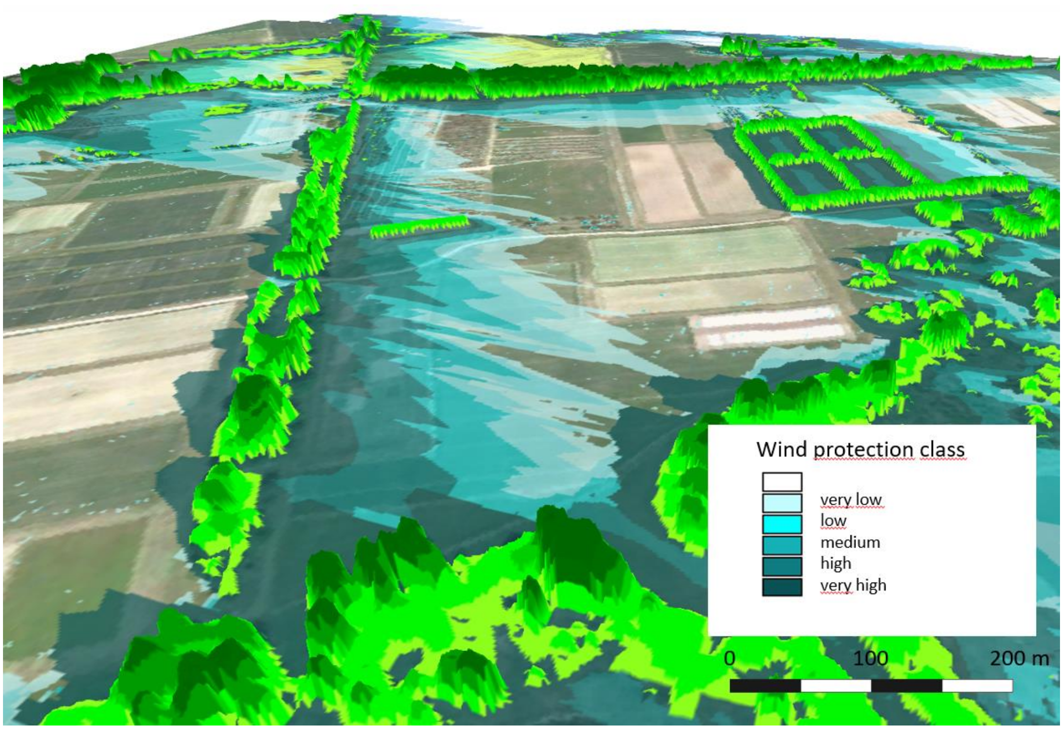

Figure 11.7. Calculated wind protection zones against wind erosion around landscape elements at the study site of Orchard Research Station, Müncheberg, Brandenburg.

The ArcGIS Toolbox WERA uses all this data to set virtual shadows that correspond to the effective protection lengths of each LE in all considered directions. To simplify the calculation procedure, the shadows are divided into five protection zones of equal length and their effect is classified from very low to very high (Table 11.2). In the final step, these protection zones are linked to the soil erodibility (Fig. 11.8). This is also available in five levels, resulting in the following the matrix in Table 11.2.

Table 11.2. Connection between soil erodibility and wind protection to derive the reduced erodibility by wind shadowing (same colours for the classes are used in Figure 11.6)

		Wind protection class				
		very low (1)	low (2)	medium (3)	good (4)	very good (5)
Soil erodibility	very low (1)	0	0	0	0	0
	low (2)	1	0	0	0	0
	medium (3)	2	1	0	0	0
	high (4)	3	2	1	0	0
	Very high (5)	4	3	2	1	0

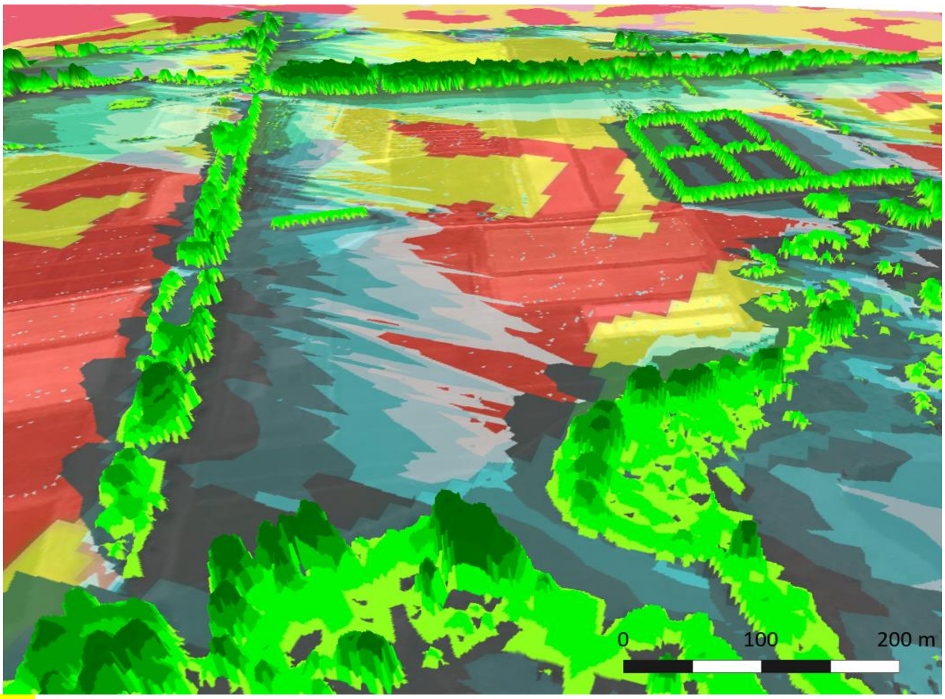

Figure 11.8. Final combination of the soil erodibility with the wind protection classes for estimation of the reduced soil susceptibility to wind erosion at the study site of Orchard Research Station, Müncheberg, Brandenburg

Derivation of parameters influencing the potential evapotranspiration

The same meteorological data were used to calculate the hourly potential evapotranspiration (PET) with a modified Penman-Equation after Wendling et al. (1991):

$$PET = g \cdot [\frac{G}{410} + (0.5 + 0.54 \cdot u_2) \cdot (100 - RH) \cdot TL/905] \quad [6]$$

With g $= 2.4 \cdot (t + 22)/(t + 123)\ldots.$

G global radiation (J cm^{-2})

u_2 wind velocity in 2 m height (m s^{-1})

RH relative humidity (%)

TL length of day (h), setting TL = 1 enables the calculation of hourly values

As the standard height for wind velocity measurements at the DWD stations is 10 m, the wind velocity for the height of 2 m is calculated with

$$u_2 = u_{10} \cdot 4.2/(3.5 + ln10) \quad [7]$$

but also any other equation for the wind profile is applicable (WMO 2012, Stull 2000).

This hourly PET values were calculated for each of the shadowed zones by reducing the wind speed by the average factors shown in Fig. 11.9. The lengths of the shadows of each direction are related to the frequencies of all measured wind velocities.

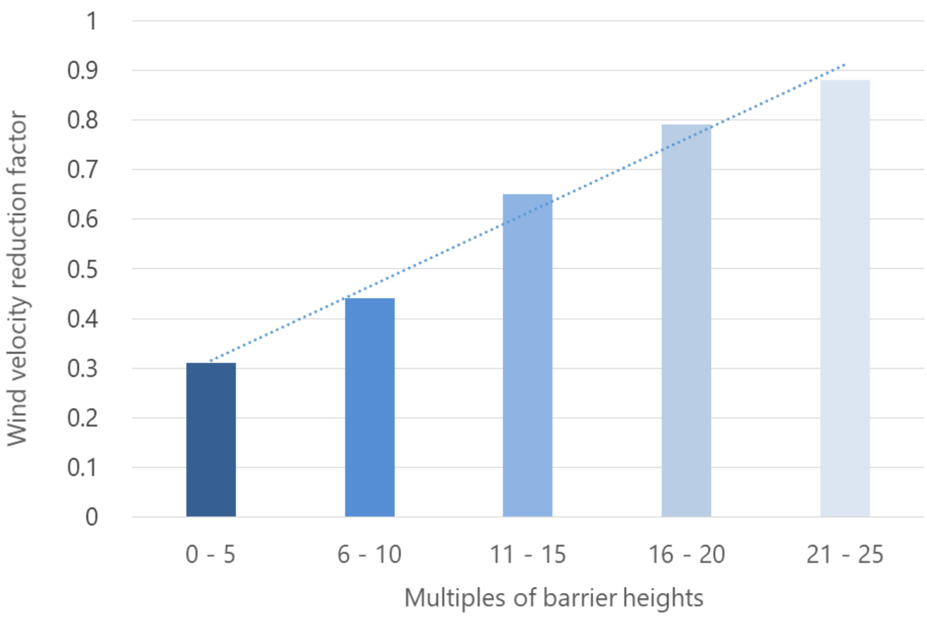

Figure 11.9. Factors of wind velocity reduction in the zones behind a landscape element, averages of the curves shown in Fig. 11.5

11.3 Regional analysis – the case study in Brandenburg

11.3.1 The study area

The study for the regional analysis is the district Märkisch-Oderland (MOL) located in the Federal State of Brandenburg, Germany. The area of MOL extends east of Berlin to the Polish border and covers 2,127 km², of which approximately 60% is used for agriculture and 23% is covered by forest (Figure 11.10). The soils originate from the Quaternary period, when large amounts of loose material were deposited during the last Ice Age. In the post-glacial period, water and wind erosion covered large areas with material sorted by the erosion processes. Ground and end moraines, alluvial fans and aeolian sands are thus the initial substrates of today's soils. As a result, there is a great variability of soils which are immediate adjacent. Soil data are available in a map from the Brandenburg State Office for Mining, Geology and Raw Materials in the scale of 1:10,000 (LGBR 2024).

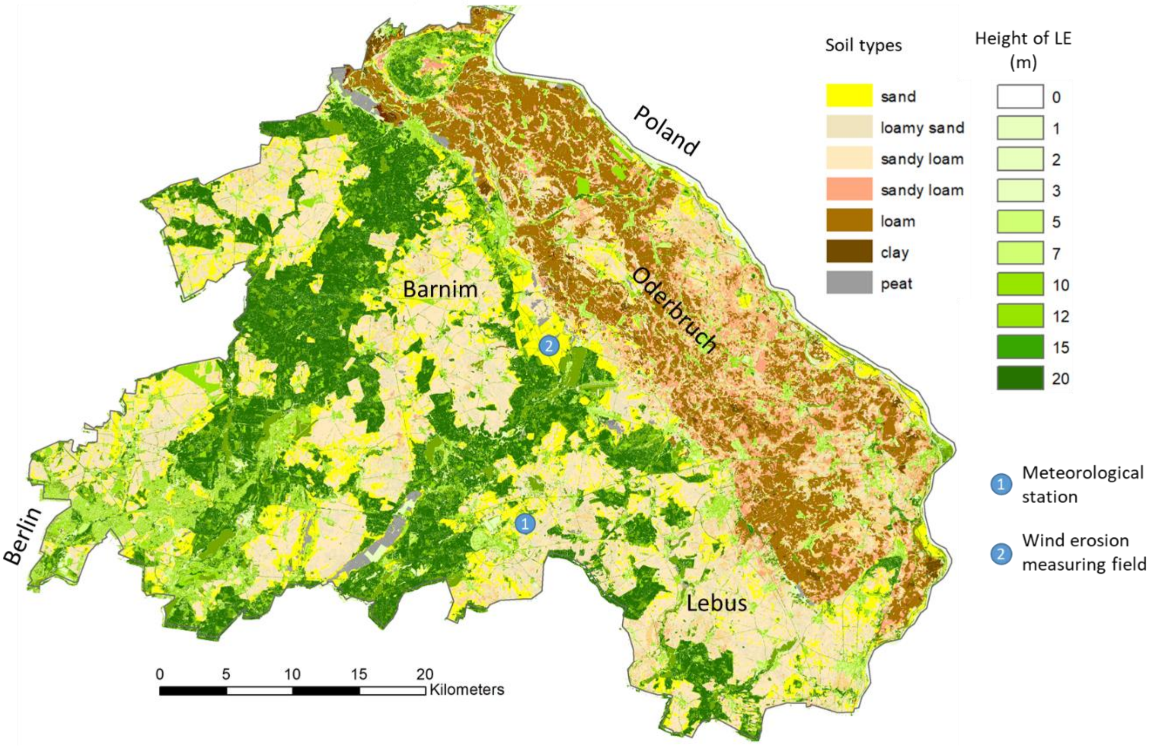

Figure 11.10. The district Märkisch-Oderland (MOL) with the main soil types on arable land and all landscape elements (LE) coloured according to their classified heights

Climate of the study area

The study area climate is characterized by the transition between maritime and continental influences. Especially the eastern part of Brandenburg with the Oderbruch belongs to the regions with the lowest annual precipitation (P) in Germany, with 533 mm in average with a span from 360 to 760 mm. In the 30-year average (1991 – 2020), precipitation remains almost constant, with a slight increase of 0.5 mm per year, whereas the last 10 years documents a strong decrease in precipitation of 16 mm per year. In terms of temperatures and daily hours of sunshine, MOL is at the upper limit in Germany (DWD 2022). Thus, the potential evapotranspiration (PET) is also correspondingly high. The 30-year average of PET is 866 mm, ranging with annual values from 740 to 1020 mm. The 30-years trend shows an increase in PET of 77 mm. There is a climatic water deficit (PET > P) from March to October. Based on these climatic conditions, both the protection of the soil from wind erosion and the reduction of evaporation by the LE are of great importance for a sustainable and successful agriculture.

11.3.2 Application wind erosion

The wind erosion affected area in the district MOL decrease considerably by including the wind reducing effects of landscape elements (Fig. 11.11). The comparison to the baseline situation where the erosion risk was only derived from soil data, the wind shadowing effect of the LE results in a reduction of the wind erosion risk area by one third, from 18,740 ha to 12,114 ha. This proves that the inclusion of landscape structures in the determination of the wind erosion risk is an essential part of the process. The ArcGIS Toolbox WERA is now an easy-to-use tool that is available on request.

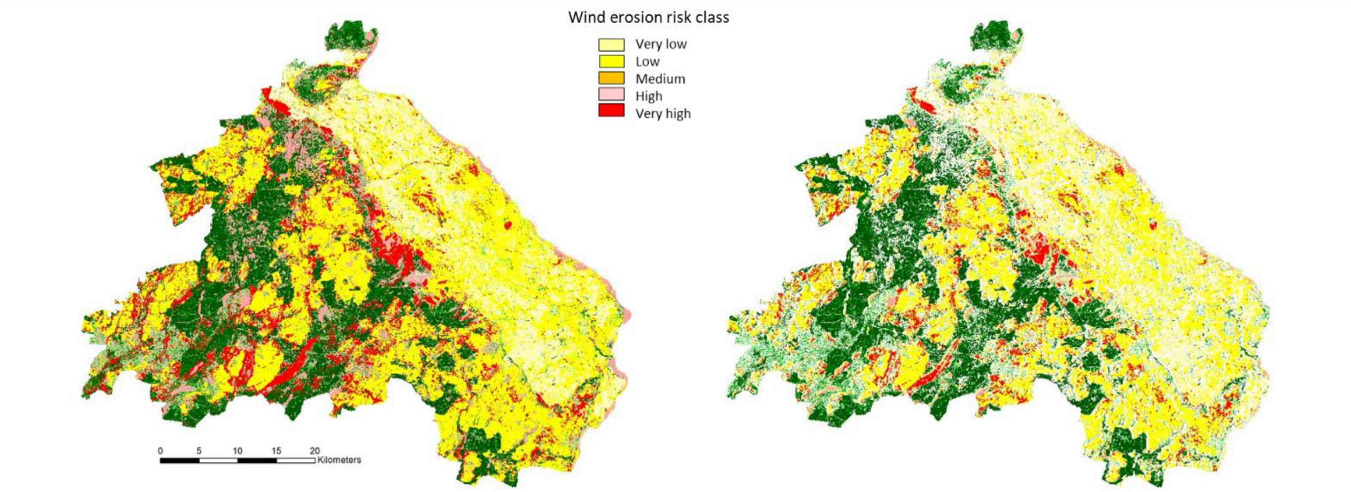

Figure 11.11. *Wind erosion risk in the county MOL, left: based on soil data, right: including wind reducing effects by landscape structures*

In addition to the regional analysis, the results can also be used as a planning tool for each individual field to optimize protective measures. The installation of new windbreak hedges can thus be adapted to the real risk potentials and scenarios for their effectiveness can be calculated over certain periods of time. The landscape section used as a case study in this chapter shows that despite the good protection provided by the hedge on the left, a significant proportion of the arable land remains in the highest risk category (Fig. 11.12). It is clear that a hedge running from north to south in the centre of the picture would be the best solution here.

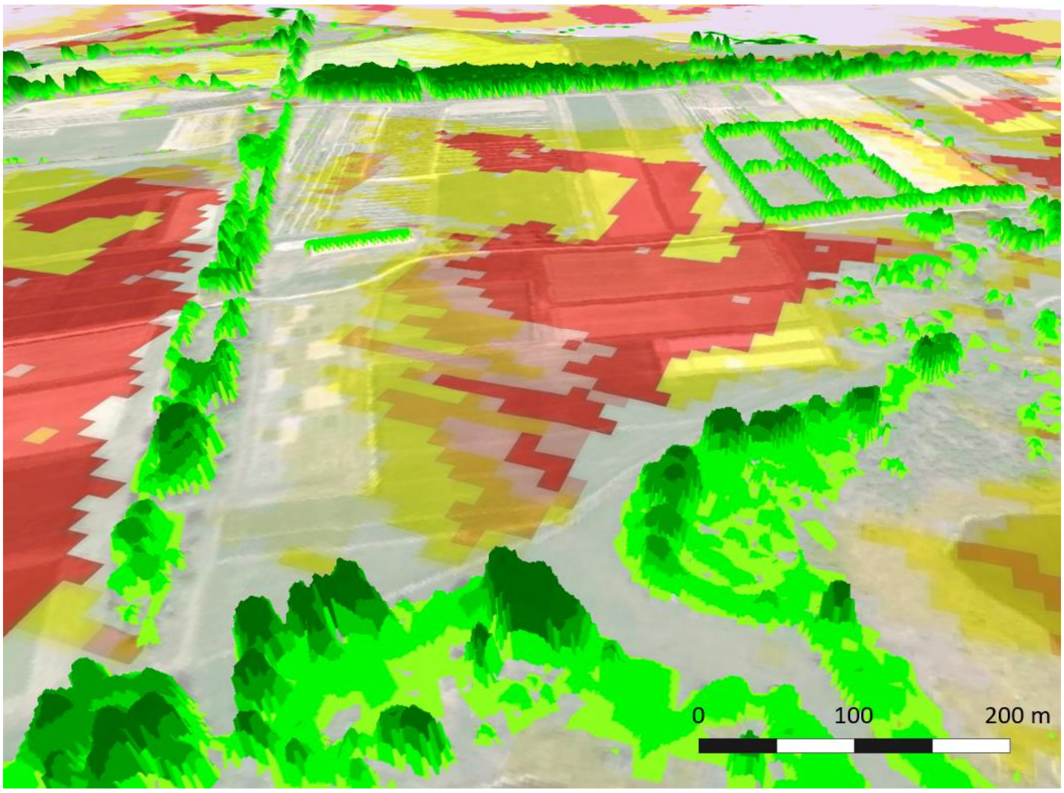

Figure 11.12. Wind erodibility resulting from the consideration of the wind-reducing effects of shelterbelts at the study site of Orchard Research Station, Müncheberg, Brandenburg (for legend see Tab. 2, Fig. 11.8)

11.4 Wind effects on the spatial distribution of the potential evapotranspiration (PET)

The reduction in wind speed also has an effect on the calculated potential evapotranspiration PET. This effect is even more pronounced in dry years (Fig. 11.13). During periods of drought, 2 - 3 days on which the plants still have sufficient water available often decide whether or not there will be serious yield losses. In the 30-years average, the annual PET is reduced to 86 % or 118 mm less PET in the zone closest to the LE, corresponding to the 0 - 5-fold of the height of each LE. With increasing distance and increasing wind velocity, the calculated evaporation increases again until it reaches its initial value again at a distance of the 20-fold of the height. These values are in good agreement with measured values from other authors (Kanzler et al. 2019, Jacobs et al. 2022). The GIS also allows these effects to be displayed in their spatial distribution (Fig. 11.14).

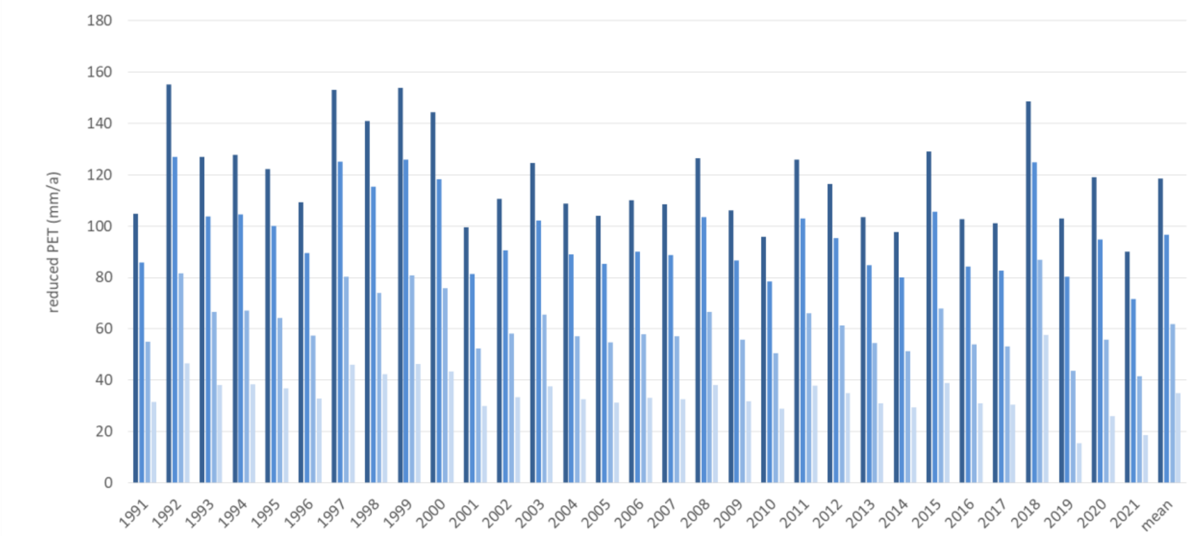

Figure 11.13. Calculated reduced Potential Evapotranspiration (PET) in the zones of wind reduction behind landscape elements (wind reduction as indicated in Fig. 11.4), dry years: 1992 (418 mm precipitation), 1999 (417 mm), 2018 (390 mm)

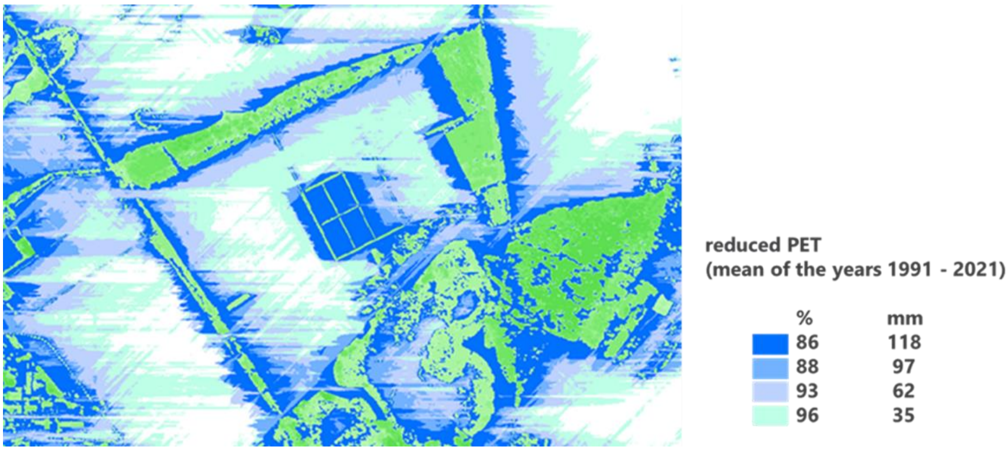

Figure 11.14 Calculated effects of the reduced wind velocities on the spatial variability of *Potential Evapotranspiration (PET)*

11.5 Conclusions

Our results support the positive effects of landscape elements on reducing wind erosion susceptibility of soils and as a potential water saving measure influencing PET. Based on state-of-the-art technologies to measure landscape structures and quantifying the protective effects of wind barriers a very detailed spatial resolution of the wind erosion risk can be derived. As the wind speed also influences the PET, the same procedure can also be used to calculate the change in PET and to quantify and visualize the effects at high spatial resolution. This is particularly important in agricultural areas with extended dry seasons, as all means should be used to prevent harmful soil degradation due to wind erosion and to minimize unproductive evaporation. Based on the results, with this powerful planning tool protection strategies can be better implemented in practice and their positive effects quantified.

Acknowledgements

The research was financed by the Federal Ministry of Education and Research (BMBF) and managed by PT-DLR as part of "*Agroforestry in Southern Africa - New pathways of innovative land-use systems under a changing climate*" (ASAP) (FKZ 01LZ1711A-F) within the framework of "*SPACES II – Science Partnerships for the Adaptation/Adjustment to Complex Earth System Processe*". Because of the SARS-Covid-19 restrictions we were not able to carry out our planned measurements in South Africa. Instead, the Orchard Research Station Müncheberg (OBVS) gave us the alternative of carrying out our measurements there to the same extent.

References

Allen RG, Pereira L, Raes D, Smith M (1998). Crop Evapotranspiration: Guidelines for Computing Crop Water Requirements. FAO Irrigation and Drainage Paper 56. Rome, Italy: Food and Agriculture Organisation.

Baade J, Aucamp I, Collett A, Eckardt F, Funk R, Glotzbach C, von Holdt J, Kestel F, Knot J, Lombard A, Morgenthal T, Msipa A, Le Roux JJ (2024). Soil erosion research and soil conservation policy in South Africa. In: von Maltitz, G.P., et al. Sustainability of Southern African Ecosystems under Global Change. Ecological Studies. Springer, Cham., pp. 335-368. https://doi.org/10.1007/978-3-031-10948-5_13

Baker TP, Jordan GJ, Baker SC (2016). Microclimate edge effects in a recently harvested forest: Do remnant forest patches create the same impact as large forest areas? Forest Ecology and Management 365: 128–136. http://dx.doi.org/10.1016/j.foreco.2016.01.022

Baker TP, Moroni MT, Hunt MA, Worledge D, Mendham D (2021) Temporal, environmental and spatial changes in the effect of windbreaks on pasture microclimate. Agricultural and Forest Meteorology 297: 1082265. https://doi.org/10.1016/j.agrformet.2020.108265

Böhm C, Kanzler M, Freese D (2014): Wind speed reductions as influenced by woody hedgerows grown for biomass in short rotation alley cropping systems in Germany. Agroforest Systems 88: 579–591. DOI 10.1007/s10457-014-9700-y

Borelli P, Balladio C, Panagos P, Montanarella L (2014). Wind erosion susceptibility of European soils. Geoderma 232–234: 471–478. https://doi.org/10.1016/j.geoderma.2014.06.008.

Borelli P, Lugato E, Montanarella L, Panagos P (2017) A new assessment of soil loss due to wind erosion in European agricultural soils using a quantitative spatially distributed modelling approach. Land Degradation and Development 28: 335–344. https://doi.org/10.1002/ldr.2588.

Brune M (2016) Urban trees under climate change. Potential impacts of dry spells and heat waves in three German regions in the 2050s. Report 24. Climate Service Center Germany, Hamburg.

Caborn JM (1957) Shelterbelts and microclimate. Forestry Commission Bulletin No. 29, Dep. Of Forestry, Edinburgh University.

Cleugh HA (1998). Effects of windbreaks on airflow, microclimates and crop yields. Agroforestry Systems 41: 55-84.

Cleigh HA, Hughes DE (2002) Impact of shelter on crop microclimates: a synthesis of results from wind tunnel and field experiments. Australian Journal of Experimental Agriculture 42: 679-701.

Funk R, Reuter HI (2006). Wind Erosion in Europe. In: Soil Erosion in Europe. Eds.: J. Boardman and J. Poesen. Wiley, London.

Funk R, Völker L, Deumlich D (2023) Landscape structure model based estimation of the wind erosion risk in Brandenburg, Germany. Aeolian Research 62: Article 100878.

Funk R, Völker L (2024). A GIS-toolbox for a landscape structure based Wind Erosion Risk Assessment (WERA). MethodsX 13: Article 103006.

Goossens D, (2004) Net loss and transport of organic matter during wind erosion on loamy sandy soil. In: Goossens, D., Riksen, M. (Eds.), Wind Erosion and Dust Dynamics: Observations, Simulations, Modelling. ESW Publications, Wageningen, pp. 81–102.

Hagen LJ, Skidmore EL, Miller PL, Kipp JE (1981) Simulation of the effect of wind barriers on airflow. Transactions of the American Society of Agricultural Engineers. 24 (4): 1002–1008.

Hagen LE, Fox FA (2020) Erosion Submodel of WEPS. In: The Wind Er, Stuttgartosion Prediction System (WEPS): Technical Documentation, J. Tatarko (Ed.). USDA Agriculture Handbook 727: 85-157. United States Department of Agriculture, Agricultural Research Service, Beltsville, MD.,

Horton R, Horn R, Bachmann J, Peth S. (eds) (2016) Essential Soil Physics. Schweizerbart Science Publisher.

Hohenbrink TL, Lischeid G (2014). Texture-depending performance of an in situ method assessing deep seepage. Journal of Hydrology 511: 61–71. http://dx.doi.org/10.1016/j.jhydrol.2015.02.

IPCC 2021. https://www.ipcc.ch/report/ar6/wg1/downloads/report/IPCC_AR6_WGI_SPM.pdf

Jacobs SR, Webber H, Niether W, Grahmann K, Lüttschwager D, Schwartz C, Breuer L, Bellingrath-Kimura SD (2022) Modification of the microclimate and water balance through the integration of trees into temperate cropping systems. Agricultural and Forest Meteorology 323: Article 109065. https://doi.org/10.1016/j.agrformet.2022.109065

Kanzler M, Böhm C, Mirck J, Schmitt D, Veste M (2019) Microclimate effects on evaporation and winter wheat (*Triticum aestivum* L.) yield within a temperate agroforestry. Agroforestry Systems 93:1821–1841. https://doi.org/10.1007/s10457-018-0289-4

Kestel F, Wulf M, Funk R (2023) Spatiotemporal variability of the potential wind erosion risk in Southern Africa between 2005 and 2019. Land Degradation and Development 34(10) 34:2945. https://doi.org/10.1002/ldr.4659

LGB (2020) Landesvermessung und Geobasisinformation Brandenburg - Digital Elevation Model of Brandenburg. https://geobasis-bb.de/lgb/de/geodaten/3d-produkte/, last access: 07.11.2024.

LGB (2023) Landesvermessung und Geobasisinformation Brandenburg - Digitales Feldblock Kataster.

LGBR (2024) Federal Service for Mining, Geology and Resources. Maps of the LBGR: http://www.geo.brandenburg.de/lbgr/

Nerger R, Funk R, Cordsen E, Fohrer N (2017) Application of a modelling approach to designate soil and soil organic carbon loss to wind erosion on long-term monitoring sites (BDF) in Northern Germany. Aeolian Research 25: 135–147.

Pásztor L, Négyesi G, Laborczi A, Kovács T, László E, Bihari Z (2016). Integrated spatial assessment of wind erosion risk in Hungary. Nat. Hazards Earth Syst. Sci. 16 (11): 2421–2432.

Plate EJ (1971) The aerodynamics of shelterbelts. Agr. Meteorol., 8: 203-222.

Řeháček D, Khel T, Kučera J, Vopravil J, Petera M (2017) Effect of windbreaks on wind speed reduction and soil protection against wind erosion. Soil and Water Research 12: 128–135. doi: 10.17221/45/2016-SWR

Reich P, Eswaran H, Beinroth F (2001) Global dimensions of vulnerability to wind and water erosion. In: Scott DE, Mohtar RH, Steinhardt GC (eds.) Sustaining the Global Farm. Selected papers from the 10th International Soil Conservation Organization Meeting held May 24-29, 1999 at Purdue University and the USDA-ARS National Soil Erosion Research Laboratory, 838-846.

R˜ tter RP, Nkomo, M, Meyer zu Drewer J, Veste M (2024) Agricultural Land-Use Systems and Management Challenges. In: von Maltitz GP, Midgley GF, Veitch J, Brümmer C, Rötter RP, Viehberg, FA, Veste M (eds) Sustainability of southern African ecosystems under global change: Science for management and policy interventions. Ecological Studies 248, Springer Nature, Cham, 551-586.

Sheppard JP, Bohn Reckziegel R, Borrass L, Chirwa PW, Cuaranhua CJ, Hassler SK, Hoffmeister S, Kestel F, Maier R, Mälicke M, Morhart C, Ndlovu NP, Veste M, Funk R, Lang Seifert F, du Toit TB, Kahle HP (2020)

Agroforestry: an appropriate and sustainable response to a changing climate in Southern Africa? Sustainability 12(17): 6796.

Schmidt M, Jochheim H, Kersebaum K-C, Lischeid G, Nendel C (2017) Gradients of microclimate, carbon and nitrogen in transition zones of fragmented landscapes—A review. Agric. For. Meteorol. 232: 659–671. http://dx.doi.org/10.1016/j.agrformet.2016.10.022

Schmidt M, Nendel, C, Funk R, Mitchell MGE, Lischeid G (2019) Modeling yields response to shading in the field-to-forest transition zones in heterogeneous landscapes. Agriculture 9, 6. https://doi.org/10.3390/agriculture9010006

Schmidt R, Deumlich D, Reuter HI (2004) From point over regions to the landscape - spatial generalization in the soil landscape research. Archives of Agronomy and Soil Science 50/3: 241-257. DOI:10.1080/03650340410001663819

Schwartz RC, Fryrear DW, Harris BL, Bilbro JD, Juo ASR (1995). Mean flow and shear stress distributions as influenced by vegetative windbreak structure. Agric. For. Meteorol. 75: 1-22.

Snyder RL, Pedras C, Montazar A, Henry JM, Ackley D (2015) Advances in ET-based landscape irrigation management. Agric. Water Manag., 147: 187-197. https://doi.org/10.1016/j.agwat.2014.07.024

Stull RB (2000) Meteorology for Scientists and Engineers. Second Edition, Brooks/Cole, Thomson Learning, USA.

van Eimern J (1964) Untersuchungen über das Klima in Pflanzenbeständen als Grundlage einer agrarmeteorologischen Beratung, insbesondere für den Pflanzenschutz. Berichte des Deutschen Wetterdienstes 96, 76 pp.

Veste M, Littmann T, Kunnecke A, du Toit B, Seifert T (2020) Windbreaks as part of climate-smart landscapes reduce evapotranspiration in vineyards, Western Cape Province, South Africa. Plant Soil Environments 66: 119–127. https://doi.org/10.17221/616/2019-PSE

Veste M, Sheppard JP, Abdulai I, Ayisi KK, Borrass L, Chirwa PW, Funk R, Kapinga K, Morhart K, Mwale SE, Ndlovu NP, Nyamadzaw G, Nyoka BI, Sebola P, Seifert T, Senyolo MP, Sileshi GW, Syampungani S, Kahle H-P (2023) The need for sustainable agricultural land-use systems: benefits from integrated agroforestry systems. In: von Maltitz GP, Midgley GF, Veitch J, Brümmer C, Rötter RP, Viehberg, FA, Veste M (eds) Sustainability of southern African ecosystems under global change: Science for management and policy interventions. Ecological Studies 248, Springer Nature, Heidelberg, pp 587–62. https://doi.org/10.1007/978-3-031-10948-5_21

Vigiak O, Sterk G, Warren A, Hagen LJ (2003) Spatial modeling of wind speed around windbreaks. Catena 52: 273-288. doi:10.1016/S0341-8162(03)00018-3

Wendling U, Schellin H-G, Thomä M (1991). Bereitstellung von täglichen Informationen zum Wasserhaushalt des Bodens für die Zwecke der agrarmeteorologischen Beratung. Zeitschrift für Meteorolologie 41: 468-475.

Weninger T, Gartner K, Riedel S, Scheper S, Michel K (2022) Der Windschutzeffekt von Bodenschutzanlagen am Beispiel Marchfeld. Österreichische Wasser- und Abfallwirtschaft74: 251–257. https://doi.org/10.1007/s00506-022-00851-y

WMO (2012). Technical Regulations, Volume I – General Meteorological Standards and Recommended Practices, 2011 edition, updated 2012, WMO-No. 49.

Zhao C, Zhang H, Wang M, Jiang H, Peng J, Wang Y (2021) Impacts of climate change on wind erosion in southern Africa between 1991 and 2015. Land Degradation & Development, 32, 2169–2182. https://doi.org/10.1002/ldr.3895

Zolina O, Simmer C, Belyaev K, Gulev SK, Koltermann P (2013) Changes in the duration of European wet and dry spells during the Last 60 Years. J. Clim. 26: 2022–2047.